Wang, H. M., Pettigrew, D. W., & Sodek, J. (1978) *Biochim. Biophys. Acta 533*, 270.
Welgus, H. G., Jeffrey, J. J., Stricklin, G. P., Roswit, W. T., & Eisen, A. Z. (1980) *J. Biol. Chem. 255*, 6806.
Welgus, H. G., Jeffrey, J. J., & Eisen, A. Z. (1981) *J. Biol. Chem. 256*, 9511.
Welgus, H. G., Jeffrey, J. J., Stricklin, G. P., & Eisen, A. Z. (1982) *J. Biol. Chem.* (in press).

Small-Angle X-ray Scattering Study of Halophilic Malate Dehydrogenase†

M. H. Reich, Z. Kam, and H. Eisenberg*

ABSTRACT: Malate dehydrogenase from the organism *Halobacterium marismortui* was studied in solutions of varying salt concentration by using a small-angle X-ray system employing a linear position sensitive detector. Considerations pertaining to the study of absorbing multicomponent solutions are presented. The radius of gyration of halophilic malate dehydrogenase was found to be 31.8 ± 0.6 Å and the shape of the molecule spheroidal. The scattering from prolate ellipsoids of eccentricity between 1 and 2 best fitted the data while for oblate ellipsoids the scattering was best fitted for eccentricities between 1 and 0.5. No significant change in the radius of gyration or anisotropy of halophilic malate dehydrogenase was found in the range of NaCl concentrations studied (1–4 M). The contrast matching electron density was found to be 0.407 ± 0.002 e/Å^3. A parallel study of bovine serum albumin yielded within experimental error a similar contrast matching electron density of 0.404 ± 0.006 e/Å^3. This information combined with the diffusion coefficient and the amount of water and salt associated with halophilic malate dehydrogenase renders the existence of an outer hydration shell unlikely. The data are rather consistent at low resolution with a spheroidal particle of uniform electron density.

Halophilic organisms provide an interesting example of biological adaptation to extreme conditions. Much interest has centered around the mechanism by which halophilic enzymes function in the extreme salinity of the intracellular medium of halobacteria (the intracellular salt concentration exceeds 4 M KCl and 2 M NaCl). Most nonhalophilic enzymes cannot function under such conditions while the halophilic enzymes are inactivated at ionic strengths typical of normal intracellular environments. The unusual behavior of halophilic enzymes leads to the expectation that their structure has characteristic and possibly unique features. The amino acid composition of halophilic malate dehydrogenase reveals a greater than usual excess of acidic amino acid residues (16–18 mol % compared with 7–9 mol % for nonhalophilic proteins), a higher content of borderline hydrophobic amino acids (alanine and threonine), and an unusually high ratio of lysine to arginine (Mevarech et al., 1977).

Malate dehydrogenase is an enzyme that catalyzes the reaction of L-malate with NAD to form oxaloacetate and NADH. Nonhalophilic malate dehydrogenase is a dimer consisting of identical subunits and has a molar mass (M_2) of between 60 000 and 72 000 g/mol for various species. Malate dehydrogenase from *Halobacterium marismortui* is also a dimer, of molar mass 85 000 g/mol. Thermodynamic analysis of contrast variation studies by analytical ultracentrifugation and quasi-elastic light scattering (Eisenberg, 1976) have shown an unusual degree of water and salt interaction with halophilic malate dehydrogenase (Pundak & Eisenberg, 1981; Pundak et al., 1981). Large amounts of water and salt were found to be associated to halophilic malate dehydrogenase (for water, 0.8 g/g of protein; for salt, 0.3 g/g of protein). For comparison, a similar study of water and sodium chloride association to bovine serum albumin found only 0.24 g of water/g of protein and 0.01 g of salt/g of protein associated (Eisenberg et al., 1978).

It has recently been reemphasized (Eisenberg, 1981) that information derived from the analysis of the intensity of zero-angle (forward) scattering, independent of the type of the incident radiation employed, is equivalent to the information derived from the ultracentrifuge. However, from the angular dependence of the scattering, additional information about macromolecular structure in solution may be obtained. Small-angle X-ray scattering in particular can be used to determine a hierarchy of basic structural information about proteins in solution. From the change in zero-angle intensity as the solvent electron density is changed, the dependence of the electron density increment of the protein on the above parameter may be derived. This is entirely analogous to the study of the mass density increment by ultracentrifugation and may be similarly analyzed. The next most accessible quantity that can be measured from the scattering at low angles is the electronic radius of gyration, which may also depend upon the electron density contrast. Further information about the shape of the molecule can be obtained at higher angles by fitting the scattering intensity to the theoretical scattering curves from simple models as ellipsoids of rotation of varying eccentricity. Procedures (Glatter, 1979) relying on the analysis of the scattering curves over the whole angular range, and the fitting of more detailed models (Pilz et al., 1975; Serdyuk et al., 1979), may be applied. In this work, we have confined ourselves to the lower resolution structural features.

X-ray scattering measurements were made of halophilic malate dehydrogenase in buffers of varying NaCl concentrations (1–4 M) and at different protein concentrations. The range of protein concentrations depended upon the salt concentration of the buffer as it proved difficult to measure the scattering from the lowest protein concentrations in the higher NaCl concentration range.

Measurements of bovine serum albumin were also made under the same conditions as the above measurements, so that a comparison of the scattering from halophilic malate dehydrogenase with a nonhalophilic protein could be made. For construction of a low-resolution model of the structure of

† From the Polymer Research Department, Weizmann Institute of Science, Rehovot, Israel. *Received March 5, 1982.*

0006-2960/82/0421-5189$01.25/0

halophilic malate dehydrogenase, measurements of the radius of gyration, R_g, the average electron density, ρ_{el}*, and the eccentricity of the best-fit ellipsoid of revolution, $p = a/b$ ($2a$ is the length of the rotation axis, and $2b$ is the length of the other two axes), were combined with information about the amount of water and salt mutually excluded. The translational diffusion coefficient, D, of this model was calculated and compared with the experimentally measured diffusion coefficient from quasi-elastic light scattering experiments. The compatibility of these data with models proposing large-scale partitioning of water and protein is examined.

Materials and Methods

Materials. Halophilic malate dehydrogenase was extracted from *Halobacterium marismortui.* The procedure of extraction, purification, and concentration determination is outlined elsewhere (Pundak & Eisenberg, 1981). Bovine serum albumin was obtained in a crystalline and lyophilized form from Sigma (no. A-4378, lot 67C-8165). Halophilic malate dehydrogenase concentration was determined by UV absorption with $A^{0.1\%}_{280nm} = 0.802$. The concentration of bovine serum albumin samples was determined by UV absorption at 279 nm by using $A^{0.1\%}_{279nm} = 0.667$ (Sterman & Foster, 1956).

The diffusion coefficient D and molar mass of the bovine serum albumin samples were measured by using quasi-elastic light scattering to check for aggregation.

Measurements of halophilic malate dehydrogenase were performed in buffers of different salt concentrations all of which contained 50 mM phosphate, adjusted to pH 7. For 4, 3, and 2 M NaCl buffers, halophilic malate dehydrogenase was dialyzed against the respective buffers while for 1.5 and 1 M buffers the enzyme was diluted from a stock solution in 4 M NaCl. Bovine serum albumin was dissolved in buffers of varying NaCl molarity in the range 1–4 M containing 0.1 M sodium acetate adjusted to pH 5.3.

X-ray Scattering. The X-ray source was a fine-focus Philips copper X-ray tube. Line focus was used so that the focus dimensions were 0.4 × 8 mm. As the beam takeoff angle is 6° with respect to the anode, the apparent focus as seen by the detector was 0.04 × 8 mm. The X-ray beam was partially monochromatized by a nickel filter which reduced the intensity of CuK_β and the continuous background intensity. Beam collimation was provided by a mirror focusing device of the Franks type using an uncoated quartz mirror (Franks, 1955) which also gave further monochromatization. A series of slits between the mirror focusing device and the sample holder was used to reduce parasitic scattering. Beam height collimation was provided by two 4-mm-high slits 32 cm apart, one just after the source and the other at the sample holder. The detector aperture height was also 4 mm. The measured half-width at half-height of the vertical divergence was approximately 14 mrad. Samples were contained in a 1-mm quartz Mark capillary.

The scattered X-rays were detected by using a position-sensitive delay line detector (Birk et al., 1976). The detection gas was a mixture of 96.5% argon and 3.5% CO_2 at a pressure of 8 atm, and the high voltage applied was 3.8 kV. The resolution of the detector was 0.3 mm. The sample to detector distance was 48 cm. The beam width at the detector was also about 0.3 mm, giving a resolution of about 0.5 mrad. Data were collected in the range of scattering angles $2\theta = 2.1$–50 mrad, corresponding to Bragg spacings [$d = \lambda/(2\theta)$] of 730–30 Å and values of q^2 [$q = (4\pi/\lambda) \sin\theta$ where λ is the wavelength] of 7.3×10^{-5} to 4.2×10^{-2} Å^{-2}.

Data were accumulated and histogrammed by using a Z-80 microcomputer system. At the conclusion of the experiment, the data were sent to an IBM 370 computer for data analysis and model-fitting calculations. The deconvolution of the data for beam height effects was performed by using the Lake procedure (Lake, 1967). The position and intensity of the primary beam were monitored by means of a semitransparent nickel beam stop. Drift of the primary beam was corrected for by shifting the histogrammed data according to the primary beam position. The effects of fluctuations in the primary beam intensity and correction for differences in absorption of X-rays by the sample (due to high NaCl concentrations) were taken into account by dividing the scattered counts in each channel by the average counts (over the experiment) of the attenuated transmitted primary beam. The scattered intensity ratios, $\tilde{I}(q)$, thus obtained incorporate all geometric instrumental factors in addition to factors including the beam intensity and the attenuation due to sample absorption. This procedure is legitimate because, at low angles of scattering, the scattered and direct beams traverse approximately the same path length through the sample (Figure 1). The nomenclature used in this contribution generally follows that of Eisenberg (1981).

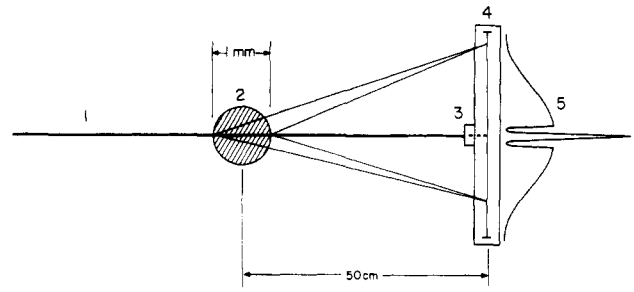

FIGURE 1: Schematic view in the detector plane of the X-ray scattering system. The capillary (2) axis is perpendicular to the position-sensitive detector (4). The semitransparent beam stop (3) allows a fraction of the primary beam (1) to pass through to the detector. A typical scattering profile (5) is shown schematically to the right of the detector.

Theory

The forward scattered intensity, $I(0)$, and the radius of gyration, R_g, are determined by applying the Guinier approximation (Guinier, 1939) to the scattering at low angles.

$$I(q) = I(0)e^{-q^2R_g^2/3} \quad (1)$$

A plot of the logarithm of the scattered intensity $I(q)$, or the experimental quantity $\tilde{I}(q)$, vs. q^2 (Guinier plot) gives a straight line at very low angles, the slope of which is $R_g^2/3$. From the intercept, $\tilde{I}(0)$ may be obtained.

The calculated scattered intensity at zero angle, $I(0)$, is given by

$$I(0) = KI_0(\partial\rho_{el}/\partial c_2)_\mu^2 M_2^* c_2 \quad (2)$$

$(M_2^*)^{-1} = M_2^{-1} + 2A_2c_2 + \ldots$, where A_2 is the second virial coefficient, $(\partial\rho_{el}/\partial c_2)_\mu$ is the electron density increment for multicomponent systems (Eisenberg, 1981), I_0 is the intensity of the unattenuated primary beam, and K is given by

$$K = i_t/(r^2N_A)$$

Here i_t is Thomson's constant for the scattering of an electron, r is the sample to detector distance, and N_A is Avogadro's number. In practice, we determine $\tilde{I}(0)$ and KI_0 in eq 2 is replaced by a constant, $\tilde{K}$, which is determined by calibration (for a given experimental configuration) by secondary standards such as a solution of particles of known molecular weight, concentration, and electron density increment. In this case, we have used solutions of bovine serum albumin of known concentration, and the electron density increments were cal-

culated from experimentally determined density increments for bovine serum albumin (Eisenberg et al., 1978) by using (Eisenberg, 1981)

$$(\partial\rho_{el}/\partial c_2)_\mu = l_2 - [(l_1 - l_3)/(1 + w_3)]\xi_3 - (l_1 + w_3 l_3)[1 - (\partial\rho/\partial c_2)_\mu]/(1 + w_3) \quad (3)$$

where l_1, l_2, and l_3 are the number of electrons per gram of water, protein, and salt, respectively, w_3 is the weight molality of salt, gram per gram of water, ξ_3 is the preferential interaction parameter for salt expressed in grams of salt per gram of protein, and $(\partial\rho/\partial c_2)_\mu$ is the mass density increment of the protein component. The calculation is not sensitive to the precise value of ξ_3. In the absence of added salt, it reduces to the simpler expression

$$d\rho_{el}/dc_2 = l_2 - l_1[1 - (d\rho/dc_2)] \quad (4)$$

If the electron density increments for the protein studied are then calculated at each salt concentration from the density increments, as above, the molar mass can be obtained from the zero-angle scattering (normalized to protein concentration) on an absolute scale, and without any model assumptions.

We now introduce model considerations to discuss interactions with water and salt. For a three-component system, we define (Eisenberg, 1976) a particle (component 2) with which are associated B_1 grams of water (component 1) per gram of particles and $B_3' = B_3 - E_3$ grams of salt (component 3) per gram of particles (E_3 refers to Donnan exclusion for charged particles). The model parameters B_1 and B_3' are related to the preferential interaction parameter ξ_3 by

$$\xi_3 = B_3' - w_3 B_1$$

If, and only if, B_1 and B_3' are independent of solvent density, determined by NaCl concentration in the present case, then we may redefine the protein component 2 to constitute an "invariant" (Luzzati et al., 1976) particle. If the solvent electron density, ρ_{el}^0, is varied and the scattering particle is invariant, the square root of the zero-angle intensity (for constant protein concentration) should vary linearly with the solvent electron density (Ibel & Stuhrmann, 1975). The solvent electron density for which the zero-angle intensity is zero is known as the matching electron density and is equal to the ρ_{el}^* of the scattering particle. In our nomenclature (Eisenberg, 1981)

$$[\tilde{I}(0)/c]^{1/2} = \tilde{K}^{1/2}M^{1/2}[(l_2 + l_1B_1 + l_3B_3') - \rho_{el}^0(\bar{v}_2 + B_1\bar{v}_1 + B_3\bar{v}_3)] \quad (5)$$

and

$$\rho_{el}^* = \frac{l_2 + l_1B_1 + l_3B_3}{\bar{v}_2 + B_1\bar{v}_1 + B_3'\bar{v}_3} \quad (6)$$

where $\bar{v}_1$, $\bar{v}_2$, and $\bar{v}_3$ are the partial specific volumes of the water, protein, and salt components, respectively. We see that linearity of $[I(0)/c]^{1/2}$ with ρ_{el}^0 for the invariant particle also requires the $\bar{v}_i$ values to be constant. This condition is usually not strictly true.

Measurements of R_g at different solvent electron densities can provide information about the internal electron density distribution. From the theory of contrast variation, R_g as a function of contrast can be written (Ibel & Stuhrmann, 1975) for an invariant particle as

$$R_g^2 = R_g'^2 + \alpha/\rho - \beta/\rho^2 \quad (7)$$

where R_g' is the radius of gyration at infinite contrast, ρ is the contrast which is the difference between the average electron density of the particle and the solvent electron density, and α and β are terms that depend on the distribution of electron density inside the scattering particle. α is positive when the electron density is larger in the outer region of the particle than in the inner and is negative for the opposite case. The term β indicates the distance between the centers of mass of different electron density regions; β vanishes when these centers coincide.

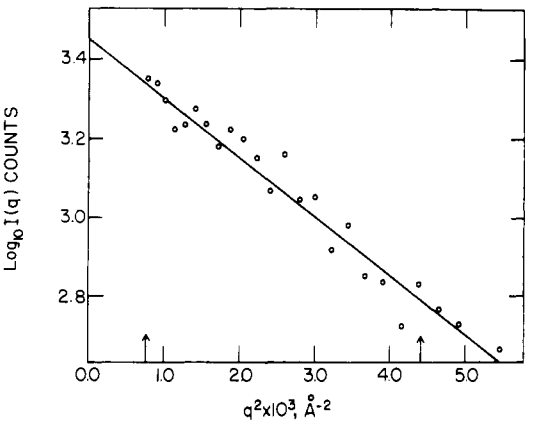

FIGURE 2: Typical Guinier plot for halophilic malate dehydrogenase in 1 M NaCl buffer. Also shown is the best-fit straight line to the data in the angular region indicated by the arrows.

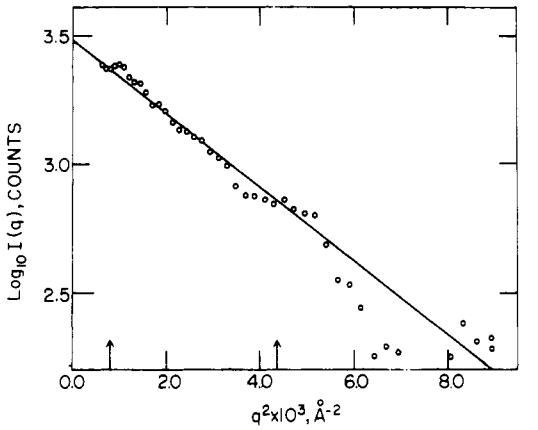

FIGURE 3: Typical Guinier plot for halophilic malate dehydrogenase in 4 M NaCl buffer. Also shown is the best-fit straight line to the data in the angular region indicated by the arrows.

The scattering from an ellipsoid of rotation was calculated by using the following equation (Guinier, 1939):

$$I(q) = \int_0^{\pi/2} \phi^2(qb\sqrt{\cos^2\omega + p^2\sin^2\omega})\cos\omega\, d\omega \quad (8)$$

where

$$\phi^2(X) = \frac{9\pi}{2}\left[\frac{J_{3/2}(X)}{X^{3/2}}\right]^2 = \left(3\frac{\sin X - X\cos X}{X^3}\right)^2$$

$J_{3/2}$ is the Bessel function of order $^3/_2$.

The effect of concentration dependence can be reduced if measurements are made over a range of protein concentrations and the measurements are extrapolated to zero protein concentration.

Results and Discussion

Shown in Table I are the measured values of the radius of gyration derived from Guinier plots at low scattering angles (Figures 2 and 3), the zero-angle intensity normalized for concentration, $\tilde{I}(0)/c$, and the best-fit eccentricity of the respective prolate and oblate ellipsoids (p_{prol} and p_{obl}) for solvent NaCl concentrations in the range 1–4 M. The measurements for 1 and 1.5 M were made within 1 and 4 h, respectively, of

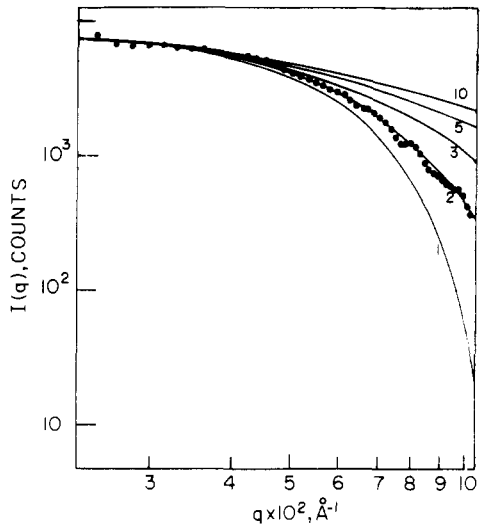

FIGURE 4: Typical experimental scattering curve for halophilic malate dehydrogenase (dots) in a 1.5 M NaCl buffer on a log I vs. log q plot. Superimposed are the theoretical scattering curves for prolate ellipsoids of varying eccentricity (solid lines) and the experimentally determined R_g.

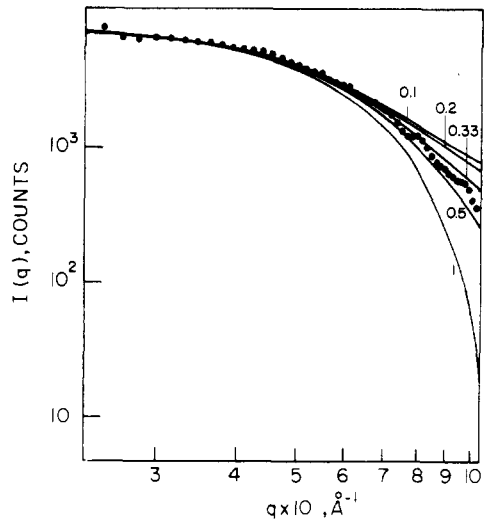

FIGURE 5: Typical experimental scattering curve for halophilic malate dehydrogenase (dots) in a 1.5 M NaCl buffer on a log I vs. log q plot. Superimposed are the theoretical scattering curves for oblate ellipsoids of varying eccentricity (solid lines) and the experimentally determined R_g.

dilution of the sample so that denaturation should be negligible (Pundak et al., 1981). The measured values of R_g for halophilic malate dehydrogenase varied between 30.1 and 34.0 Å over all the measurements. The average value of R_g was 31.8 ± 0.6 Å. If all the R_g values at all salt concentrations are placed on a R_g against concentration plot, some concentration dependency appears, and at infinite dilution, R_g equals 32.7 Å. The correlation coefficient $r = -0.39$ indicates rather poor correlation. Because of the weak scattering intensities, due to absorption of X-rays by the salt buffer and the low electron density contrast between the protein and buffer, the measurements were subject to experimental "noise", and the relatively small changes in R_g are probably not significant. Thus, least-squares analysis of the variation of R_g with contrast (eq 7) gave the value of 5.3×10^{-5} for α with a large standard deviation of 9.3×10^{-5}. This value, though similar to that reported for myoglobin (Ibel & Stuhrmann, 1975), does not have much statistical significance. It is much smaller than values reported for molecules known to contain regions of greatly differing scattering density such as ferritin (Stuhrmann & Duee, 1975) and lipoprotein (Stuhrmann et al., 1975). In the present context, it becomes meaningless to analyze the data for β.

Using the value of $\tilde{K}$ calculated as described above and the electron density increments (Table I) calculated from the values for ξ_1 (which is equal to $-\xi_3/w_3$) and $(\partial\rho/\partial c_2)_\mu$ for halophilic malate dehydrogenase given in Pundak & Eisenberg (1981), we found (Table I) the average value of the molar mass of halophilic malate dehydrogenase, over all the measurements, to be 77 600 ± 10 300 g/mol. This is in reasonable agreement with the more accurate laser light scattering value of 85 000 ± 1200 g/mol previously reported (Pundak & Eisenberg, 1981). The study of biological molecules in high salt concentration is a difficult system for the evaluation of X-ray scattering data, and the calculation is undertaken to demonstrate that even under difficult conditions, it is possible to obtain reasonable data on an absolute scale.

Figures 4 and 5 show a typical scattering curve for halophilic malate dehydrogenase with the theoretical scattering from ellipsoids of varying eccentricity superimposed. p_{prol} varied between 1 and 2 and p_{obl} between 1 and 0.33 over all the measurements. The average values of p_{prol} and p_{obl} were 1.7 and 0.61, respectively. Again, no systematic trend with the salt concentration of the buffer can be discerned. For bovine serum albumin, R_g also did not change significantly with changes in the salt concentration of the buffer. The average R_g was 29.3 ± 0.7 Å, and the average best-fit eccentricities were 2.5 for the prolate ellipsoid and 0.36 for the oblate ellipsoid.

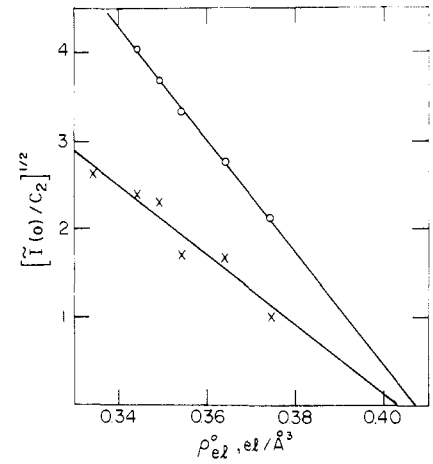

FIGURE 6: Reduced scattering intensity, $[\tilde{I}(0)/c]^{1/2}$ (in arbitrary units), vs. solvent electron density, ρ_{el}^0, for halophilic malate dehydrogenase (circles) and bovine serum albumin (crosses). Also shown are the best-fit straight lines to the halophilic malate dehydrogenase and bovine serum albumin data.

In Figure 6 a plot of $[\tilde{I}(0)/c]^{1/2}$ vs. solvent electron density is shown for halophilic malate dehydrogenase and for bovine serum albumin. As the $\tilde{I}(0)/c$ measurements do not display any consistent concentration dependence, the average (cf. Table I) of $\tilde{I}(0)/c$ for each solvent electron density was plotted. Within the error of the experiments, the data in Figure 6 lie on a straight line. The best-fit straight lines intercept the $[\tilde{I}(0)/c]^{1/2} = 0$ axis at solvent electron densities of 0.407 ± 0.002 e/Å^3 for halophilic malate dehydrogenase and 0.404 ± 0.006 e/Å^3 for bovine serum albumin. If the invariant particle hypothesis is assumed (Luzzati et al., 1976), then these values correspond to the average electron densities of the scattering particles. The experimental ratio of the two slopes in Figure 6 is 1.6 ± 0.3. From eq 5, we calculate (assuming an average

Table I: Experimental Results and Calculated Quantities for Halophilic Malate Dehydrogenase

[NaCl] (M)	c_2 (mg/mL)	R_g (Å)	$\tilde{I}(0)/c$	p_{prol}	p_{obl}
1.0	5.05	32.0	17.9	1.5	0.67
	7.70	30.4	17.4	1.0	1.00
	11.5	32.9	12.2	2.0	0.50
	17.8	31.2	17.7	1.5	0.67
		31.4 ± 0.9 [a]	16.3 ± 2.3 [a]	1.5 ± 0.4 [a]	0.71 ± 0.18 [a]
		$(\partial\rho_{el}/\partial c_2)_\mu = 1.14 \times 10^{23}$ e/g; M_2 = 70 300 g/mol			
1.5	7.50	31.4	14.9	2.0	0.50
	8.50	34.0	12.5	2.5	0.20
		32.7 ± 1.3 [a]	13.7 ± 1.2 [a]	2.3 ± 0.3 [a]	0.35 ± 0.15 [a]
		$(\partial\rho_{el}/\partial c_2)_\mu = 1.06 \times 10^{23}$ e/g; M_2 = 65 000 g/mol			
2.0	8.90	31.6	12.4	1.5	0.67
	13.3	32.0	11.8	1.5	0.67
	17.8	31.2	10.2	1.5	0.67
	26.6	30.1	9.86	1.0	1.00
		31.2 ± 0.7 [a]	11.1 ± 1.1 [a]	1.4 ± 0.2 [a]	0.75 ± 0.14 [a]
		$(\partial\rho_{el}/\partial c_2)_\mu = 9.61 \times 10^{22}$ e/g; M_2 = 84 200 g/mol			
3.0	6.65	31.8	9.49	1.5	0.50
	10.0	33.0	7.52	2.0	0.33
	13.3	30.6	6.87	1.0	1.00
	26.6	30.5	6.32	1.0	1.00
		31.5 ± 1.0 [a]	7.55 ± 1.2 [a]	1.4 ± 0.4 [a]	0.71 ± 0.30 [a]
		$(\partial\rho_{el}/\partial c_2)_\mu = 7.64 \times 10^{22}$ e/g; M_2 = 74 500 g/mol			
4.0	11.8	32.5	4.75	2.0	0.50
	14.8	32.0	4.90	1.5	0.67
	17.7	33.7	3.95	2.0	0.33
	23.6	31.4	4.26	1.5	0.67
		32.4 ± 0.8 [a]	4.46 ± 0.4 [a]	1.8 ± 0.3 [a]	0.54 ± 0.14 [a]
		$(\partial\rho_{el}/\partial c_2)_\mu = 6.07 \times 10^{22}$ e/g; M_2 = 94 000 g/mol			
		31.8 ± 0.6 [b]		1.7 ± 0.3 [b]	0.61 ± 0.15 [b]
			M_2 = 77 600 ± 10 300 [b]		

[a] Average values. [b] Total average.

value for $\bar{v}_3$ of 0.35 cm³/g) a value of 1.83, using the parameters given in Table II. Similarly, from eq 6, we calculate $\rho_{el}^* = 0.411$ e/Å³ for halophilic malate dehydrogenase and 0.412 e/Å³ for bovine serum albumin. The agreement of measured and calculated values is satisfactory in view of the dissimilarity of the two systems with respect to salt and water interactions and demonstrates that parameters derived from sedimentation experiments may be used to unequivocally predict the forward scattering phenomena.

We shall now proceed to examine additional information which can be derived from the scattering experiments.

Calculation of the Volume of the Scattering Particle. The volume will be calculated independently by two different procedures: (a) from the average electron density and the total number of electrons in the particle and (b) from the best-fit ellipsoid.

The volume can be calculated from knowledge of the average electron density of the particle and the total number of electrons included in that volume:

$$V_{tot} = N_{el}/\rho_{el}^* \quad (9)$$

where V_{tot} is the volume of the protein plus associated solvent constituents and N_{el} is the total number of electrons per scattering particle. N_{el} can be easily determined from the chemical composition of the protein and from the amount of water and salt believed to be associated with the protein, i.e.

$$N_{el} = N_{el}(\text{protein}) + N_{el}(H_2O) + N_{el}(\text{NaCl}) = M_2(l_2 + l_1B_1 + l_3B_3')/N_A \quad (10)$$

where N_{el}(protein) is the number of electrons in the dry weight of the protein and $N_{el}(H_2O)$ and N_{el}(NaCl) are the respective number of electrons of the water and salt associated with the protein particle. The calculated values of V_{tot} and the number of electrons in each component are given in Table II for

Table II: Summary of the Physical Properties of Halophilic Malate Dehydrogenase and Bovine Serum Albumin

property	halophilic malate dehydrogenase	bovine serum albumin
ρ_{el}^* (e/Å³)	0.407 [a]	0.404 [a]
B_1 (g/g)	0.8 [b]	0.24 [c]
B_3' (g/g)	0.3 [b]	0.012 [c]
R_g (Å)	31.8	29.3
p_{prol}	1.7	2.5
p_{obl}	0.61	0.36
M_2 (g/mol)	85000 [b]	68000 [d]
$\bar{v}_2$ (cm³/g)	0.75 [b]	0.734 [e]
V(protein) (Å³)	105000	84000
l_2 (e/g × 10^{-23})	3.24 [f]	3.19 [g]
N_{el}(protein)	45000	36500
$N_{el}(H_2O)$	37400	9100
N_{el}(NaCl)	12100	390
N_{el}	94500	45990
V_{tot} (Å³)	232000	114000

[a] Figure 5. [b] Pundak & Eisenberg (1981). [c] Eisenberg et al. (1978). [d] Harrington et al. (1956). [e] Charlewood (1957). [f] Calculated from the chemical composition. [g] Luzzati et al. (1961). Additional quantities used in calculations in Tables I and II were the following: $l_1 = 3.343 \times 10^{23}$ e/g, $l_3 = 2.885 \times 10^{23}$ e/g, $\bar{v}_1$ = 1 cm³/g, $\bar{v}_3$ = 0.335, 0.346, 0.357, 0.374, and 0.388 cm³/g for 1, 1.5, 2, 3, and 4 M NaCl, respectively.

halophilic malate dehydrogenase and bovine serum albumin.

The volume can also be calculated from the dimensions of the uniform ellipsoid whose scattering best fits the data. The volume can be derived from R_g and p for a uniform ellipsoid from

$$V = (4\pi/3)[5R_g^2/(2 + p^2)]^{3/2}p \quad (11)$$

If the volume of the best-fit ellipsoid is similar to that calculated from the average electron density and the total number of electrons, then the assumption that the molecules have the shape of the best-fit ellipsoid and have uniform electron density is consistent. The volume of the prolate ellipsoid of uniform electron density that best fits the data (R_g = 31.8 Å and p = 1.7) is 237 000 Å^3 while the volume of the best-fit oblate ellipsoid (R_g = 31.8 Å and p = 0.61) is 254 000 Å^3. Both these volumes are close to the volume 232 000 Å^3, calculated from the average electron density and the total number of electrons. This indicates that ellipsoidal models of uniform electron density are consistent with the data. The same calculations for bovine serum albumin also indicate that an ellipsoid of uniform electron density is consistent with the data in Table II, the respective volumes being 124 000 Å^3 for the best-fit prolate ellipsoid and 136 000 Å^3 for the best-fit oblate ellipsoid, and the volume obtained from the total number of electrons and the average electron density is 114 000 Å^3. These data are in agreement with earlier X-ray studies of this protein (Anderegg et al., 1955; Luzzati et al., 1961).

Table II summarizes the results of the X-ray measurements of halophilic malate dehydrogenase as well as other relevant physical parameters. Also included for comparison are the same parameters for bovine serum albumin.

Consistency with Diffusion Measurements. Comparison of the diffusion coefficients calculated from the dimensions of the best-fit ellipsoid with the measured diffusion coefficient can also indicate whether the simple uniform density ellipsoidal models are consistent with the data. The equations for the translational diffusion coefficient of prolate and oblate ellipsoids have been derived by Perrin (1934). For halophilic malate dehydrogenase, the best-fit prolate ellipsoid had R_g = 31.8 Å and p = 1.7; therefore, the length of the semiminor axis b of an ellipsoid of such dimensions is 32.2 Å while the length of the semimajor axis a is 54.7 Å. For D, we calculate 5.4 × 10^{-7} cm^2/s. For the best-fit oblate ellipsoid (R_g = 31.8 Å and p = 0.61), b = 46.2 Å and a = 28.2 Å. For such an ellipsoid, the translational diffusion coefficient D yields 5.3 × 10^{-7} cm^2/s. These values are in reasonable agreement with the experimentally determined diffusion coefficient of (4.75–5.25) × 10^{-7} cm^2/s over the range 1–5 M NaCl (Pundak & Eisenberg, 1981).

Similarly for bovine serum albumin for the best-fit prolate ellipsoid with R_g = 29.3 Å and p = 2.5 (b = 22.8 Å, a = 57.0 Å), D was calculated to be 6.4 × 10^{-7} cm^2/s while the diffusion coefficient of the best-fit oblate ellipsoid, R_g = 29.3 Å and p = 0.36 (b = 44.9 Å, a = 16.2 Å), was calculated to be 6.2 × 10^{-7} cm^2/s. These values are also in reasonable agreement with the experimentally determined diffusion coefficient of 5.9 × 10^{-7} cm^2/s.

A Hydration Shell Is Not Consistent with the R_g Measurements. We have seen that the X-ray data presented are in agreement with the earlier findings (Pundak & Eisenberg, 1981; Pundak et al., 1981) that unusually large amounts of water and salt are associated with halophilic malate dehydrogenase when compared to a nonhalophilic protein such as bovine serum albumin, assuming a uniformly distributed particle. We will now show that the X-ray data are not consistent with a hypothesis favored by some that the extra water associated with halophilic proteins is distributed in an outside layer surrounding a normally hydrated protein core.

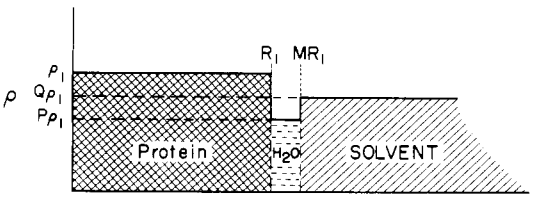

FIGURE 7: Schematic representation of the radial electron density distribution of the hydration shell model described under Results and Discussion. R_1 is the radius of the protein core, MR_1 is the radius of the protein plus hydration shell, ρ_1 is the electron density of the core, $P\rho_1$ is the electron density of the hydration shell, and $Q\rho_1$ is the electron density of the buffer.

We can calculate the radius of gyration of a particle consisting of protein surrounded by an aqueous layer in solvents of differing electron density. The radius of gyration is defined as

$$R_g^2 = \int_V \rho(r)r^2\,dV / \int_V \rho(r)\,dV$$

where $\rho(r)$ is the excess electron density distribution inside the scattering particle and V is the integral over the volume of the particle. For a spherically symmetric particle, R_g is given by

$$R_g^2 = \int_0^R \rho(r)r^4\,dr / \int_0^R \rho(r)r^2\,dr$$

where R is the radius of the particle. As halophilic malate dehydrogenase is close to spherical in shape, this approximation is permissible. The radial electron density distribution of a spherically symmetric particle, consisting of two components of electron density ρ_1 and $P\rho_1$ in a solvent of electron density $Q\rho_1$, is represented schematically in Figure 7. For this case, R_g is given by

$$R_g^2 = \frac{\int_0^{R_1}(\rho_1 - Q\rho_1)r^4\,dr + \int_{R_1}^{MR_1}(P\rho_1 - Q\rho_1)r^4\,dr}{\int_0^{R_1}(\rho_1 - Q\rho_1)r^2\,dr + \int_{R_1}^{MR_1}(P\rho_1 - Q\rho_1)r^2\,dr} = R_{g_1}^2\frac{1 - P + M^5(P - Q)}{1 - P + M^3(P - Q)} \quad (12)$$

where R_{g_1} is the radius of gyration of the region from 0 to R_1, R_1 is the radius of the protein core, and MR_1 is the radius of the protein plus hydration shell. The thickness of the hydration shell is therefore $A = R_1(M - 1)$.

For bovine serum albumin, the dry volume per particle expected from the partial specific volume and the molar mass is 84 000 Å^3 while the volume of the "scattering particle" calculated from ρ_{el}^0 and N_{el} is 114 000 Å^3 (see Table II). The increase in volume of ~35% can be attributed to the incorporation of 0.24 and 0.012 g/g of protein of water and NaCl. Scaling the volumes in the same fashion for a protein of molar mass 85 000 g/mol, corresponding to halophilic malate dehydrogenase, and assuming identical interactions with salt and water, we obtain a dry volume of 105 000 Å^3 and a water- and salt-associated volume of 144 000 Å^3 for the protein core.

For a particle of volume 144 000 Å^3 and p = 1.7, the expected R_g from the inversion of eq 11 is 26.9 Å. Taking this value for the radius of gyration of the protein core and assuming the particle is surrounded by a water layer of thickness A angstroms, we can calculate the R_g for the entire particle by using eq 12. The value of P used (0.835) is the ratio of the electron density of water (0.344 e/Å^3) to the hydrated protein electron density of the core (0.40 e/Å^3). In Table III,

Table III: R_g as a Function of Aqueous Layer Thickness (A) and Solvent NaCl Concentration As Calculated from the Hydration Model

[NaCl] (M)	A (Å)	R_g (Å)
1	0.4	26.9
	4.4	26.1
	7.6	25.1
2	0.4	26.8
	4.4	25.3
	7.6	23.0
3	0.4	26.7
	4.4	24.5
	7.6	19.8
4	0.4	26.5
	4.4	23.5
	7.6	14.4

using eq 12, the expected R_g for such a model with different values of A in buffers of differing salt concentrations is given. A uniform water layer thickness of 4.4 Å corresponds to a volume of 83 000 Å^3, which is approximately the difference between the measured volume of halophilic malate dehydrogenase (232 000 Å^3) and the volume of the core (144 000 Å^3). From Table III, it can be seen that the radius of gyration for such a model, consisting of normally hydrated protein surrounded by a water layer, should vary between 26.1 Å at 1 M NaCl and 23.5 Å at 4 M NaCl. This is not consistent with the experimentally measured radius of gyration of halophilic malate dehydrogenase which is 31.8 ± 0.6 Å (Table I) with no consistent trend as the salt concentration of the buffer was altered.

We have not included the salt distribution in the preceding calculations, even though it may significantly modify the electron density distribution, because there is no conceivable salt distribution (other than salt being included in the outside water layer, thereby negating any possible "protective" influence of the layer) that would enable the calculated radius of gyration to approach the experimental value.

Conclusions

The present small-angle X-ray scattering study thus confirms, by a variety of criteria, the observation derived from ultracentrifugation and light scattering (Pundak & Eisenberg, 1981; Pundak et al., 1981) that unsually large amounts of salt and water are associated with halophilic malate dehydrogenase in distinction to the usual proteins, for which bovine serum albumin was taken as an example. This phenomena is no doubt of major significance for maintaining the stability and activity of the halophilic enzymes at extreme concentrations of salt; yet at the resolution of the methods used to date, precise localization of the various components with the enzyme "particle" is not feasible. The vanishingly low values of the parameter α describing the inhomogeneity of the internal electron density and the consistency of uniform electron density models with the X-ray and diffusion data indicate that there is no large-scale partitioning of electron density inside the scattering particle (protein plus associated salt and water) for halophilic malate dehydrogenase. Furthermore, models of halophilic malate dehydrogenase that incorporate large amounts of water located toward the exterior of the particle are not consistent with the R_g measurements. However as the data, as stated above, can only provide "low resolution" structural information, small-scale partitioning of the electron density (such as pockets of water and salt) cannot be ruled out.

It is not possible to distinguish between prolate and oblate ellipsoids as they both fitted the X-ray scattering and diffusion data equally well. However, it may be possible to distinguish between the two models from determination of the largest molecular extension from the limits of the pair distribution function (Glatter, 1979). Furthermore, by neutron scattering the problems of working in high salt buffers, such as reduced contrast and beam absorption, can be greatly reduced. The contrast can be increased by suitable choice of the ratio of D_2O to H_2O in the buffer, and little absorption of neutrons by salt buffers is expected because of low absorption cross section for neutrons. Also a more extensive range of contrast can be explored, as the scattering length of the buffer can be changed, without altering the ionic strength, by simply changing the D_2O:H_2O ratio. Information about the rate of exchange of buffer D_2O with associated H_2O could also be obtained. It would therefore appear that a study of halophilic malate dehydrogenase by neutron scattering would provide a natural extension of the data presented here.

Acknowledgments

We are grateful to the anonymous reviewer for his helpful suggestions.

References

Anderegg, J. W., Beeman, W. W., Shulman, S., & Kaesberg, P. (1955) *J. Am. Chem. Soc. 77*, 2927–2937.

Birk, M., Breskin, A., & Trautner, N. (1976) *Nucl. Instrum. Methods 137*, 393–395.

Charlewood, P. A. (1957) *J. Am. Chem. Soc. 79*, 776–781.

Eisenberg, H. (1976) *Biological Macromolecules and Polyelectrolytes in Solution*, Oxford University Press, London.

Eisenberg, H. (1981) *Q. Rev. Biophys. 14*, 141–172.

Eisenberg, H., Haik, Y., Ifft, J., Leicht, W., Mevarech, M., & Pundak, S. (1978) in *Energetics and Structure of Halophilic Microorganisms* (Caplan, S. R., & Ginzburg, M., Eds.) pp 13–32, Elsevier/North-Holland, Amsterdam.

Franks, A. (1955) *Proc. Phys. Soc., London, Sect. B 68*, 1054–1064.

Glatter, O. (1979) *J. Appl. Crystallogr. 12*, 166–175.

Guinier, A. (1939) *Ann. Phys. (Paris) 12*, 161–237.

Harrington, W. F., Johnson, P., & Ottewill, R. H. (1956) *Biochem. J. 62*, 569–582.

Ibel, K., & Stuhrmann, H. B. (1975) *J. Mol. Biol. 93*, 255–265.

Lake, J. A. (1967) *Acta Crystallogr. 23*, 191–194.

Luzzati, V., Witz, J., & Nicolaieff, A. (1961) *J. Mol. Biol. 3*, 379–390.

Luzzati, V., Tardieu, A., Mateu, L., & Stuhrmann, H. B. (1976) *J. Mol. Biol. 101*, 115–127.

Mevarech, M., Eisenberg, H., & Neumann, E. (1977) *Biochemistry 16*, 3781–3785.

Perrin, F. (1934) *J. Phys. Radium 5*, 497–511.

Pilz, I., Kratky, O., Licht, A., & Sela, M. (1975) *Biochemistry 14*, 1326–1333.

Pundak, S., & Eisenberg, H. (1981) *Eur. J. Biochem. 118*, 463–470.

Pundak, S., Aloni, H., & Eisenberg, H. (1981) *Eur. J. Biochem. 118*, 471–477.

Serdyuk, I. N., Grenader, A. K., & Zaccai, G. (1979) *J. Mol. Biol. 135*, 691–707.

Sterman, M. D., & Foster, J. F. (1956) *J. Am. Chem. Soc. 78*, 3652–3656.

Stuhrmann, H. B., & Duee, E. D. (1975) *J. Appl. Crystallogr. 8*, 538–542.

Stuhrmann, H. B., Tardieu, A., Mateu, L., Sardet, C., Luzatti, V., Aggerbeck, L., & Scanu, A. M. (1975) *Proc. Natl. Acad. Sci. U.S.A. 72*, 2270–2273.